

Structural and Luminescent Spectroscopic Properties of Solid-solution Phosphor $\text{Ca}_x\text{Sr}_{2-x}\text{SiO}_4 : \text{Eu}^{2+}, \text{Dy}^{3+}$

WEI Wei, MAO Jiashan, JIANG Bin, CHEN Yonghu[†], YIN Min

Key Laboratory of Strongly-Coupled Quantum Matter Physics, Chinese Academy of Science, School of Physical Sciences,
University of Science and Technology of China, Hefei 230026, China

Received date: 2019-01-29; accepted date: 2018-03-05

【Abstract】 A series of divalent europium(Eu^{2+}) ions and trivalent dysprosium(Dy^{3+}) ions co-doped solid-solution $\text{Ca}_x\text{Sr}_{2-x}\text{SiO}_4$ ($x=0, 0.2, 0.4, 0.6, 0.8, 1.0, 1.2, 1.4, 1.6, 1.8, 2.0$) phosphors were synthesized by solid-state reaction and their luminescent spectroscopic properties were investigated. Photoluminescence emission spectra of $\text{Ca}_x\text{Sr}_{2-x}\text{SiO}_4 : 0.01\text{Eu}^{2+}, 0.01\text{Dy}^{3+}$ phosphor was changed by increasing the proportion of Ca^{2+} ions. Two emission bands originated from the 5d-4f transition of Eu^{2+} ion occupying two different cation sites in the $\text{Ca}_x\text{Sr}_{2-x}\text{SiO}_4$ host lattice were observed under ultraviolet excitation when $x \geq 1.2$. The red-shift of emission peaks with different Ca^{2+} and Sr^{2+} concentrations was observed when $0 < x < 1$. The maximum integrated luminescence intensity was observed for the $\text{Ca}_x\text{Sr}_{2-x}\text{SiO}_4 : 0.01\text{Eu}^{2+}, 0.01\text{Dy}^{3+}$ ($x=1.0$) phosphor under 365 nm excitation. Also this study outlines a novel approach to the synthesis of an efficient yellow-green emitting $\text{Ca}_x\text{Sr}_{2-x}\text{SiO}_4 : 0.01\text{Eu}^{2+}, 0.01\text{Dy}^{3+}$ phosphor.

Keywords: luminescent materials, solid-solution, rare-earth ions, luminescent properties

PACS: 32.50.+d

DOI: 10.13380/j.ltpl.02019.01.003

Reference method: WEI Wei, MAO Jiashan, JIANG Bin, CHEN Yonghu, YIN Min, Low. Temp. Phys. Lett. **41**, 0021 (2019)

Eu^{2+} 和 Dy^{3+} 共掺 $\text{Ca}_x\text{Sr}_{2-x}\text{SiO}_4$ 硅酸盐固溶体发光性质探究

卫 威, 毛家珊, 姜 斌, 陈永虎, 尹 民

强耦合量子物理重点实验室, 中国科学技术大学物理学院, 安徽合肥 230026

收稿日期: 2019-01-29; 接收日期: 2018-03-05

【摘要】 稀土发光材料和固溶体发光材料受到人们的广泛关注, 稀土固溶体发光材料本身的结构特性在一定程度上能够影响和决定它的发光特性, 而发光特性又直接关系到材料的性能和使用前景. 因此, 本论文的主要工作是通过改变固溶体发光材料 $\text{Ca}_x\text{Sr}_{2-x}\text{SiO}_4 : 0.01\text{Eu}^{2+}, 0.01\text{Dy}^{3+}$ 固溶离子 Ca 和 Sr 的比例浓度来实现对固溶体发光材料基质结构的调节, 测得了不同固溶比例下的样品的激发光谱和部分发射光谱以及热释光谱, 并对这些实验结果进行分析.

关键词: 发光材料, 固溶体, 稀土离子, 结构性质, 发光特性

PACS: 32.50.+d

DOI: 10.13380/j.ltpl.02019.01.003

引用方式: 卫威, 毛家珊, 姜斌, 陈永虎, 尹民, Low. Temp. Phys. Lett. **41**,0021 (2019)

[†] yhuchen@ustc.edu.cn

1 Introduction

The lanthanide ions doped luminescent materials have wide applications in many fields like lighting, display, optical sensors, bio-imaging^[1-6]. In all these applications, one crucial aspect is to obtain desired light emission within appropriate wavelength range through spectral conversion of suitable luminescent centers. The emission spectrum of Dy^{3+} consists of blue and yellow emissions among trivalent lanthanide (Ln^{3+}) ions. The $^4\text{F}_{9/2} \rightarrow ^6\text{H}_{13/2}$ transition of Dy^{3+} is very sensible and its emission intensity also strongly depends on the local lattice environment. By changing the composition of the host material, the Dy^{3+} co-doped phosphors can emit white light. On the other hand, divalent Eu^{2+} doped phosphors usually have strong absorption and excitation in the spectrum region from ultraviolet to blue due to the spin-allowed f-d transition, and their broadband emissions corresponding to the transition of $4\text{f}^65\text{d}^1 \rightarrow 4\text{f}^7$ are also host specific because the electron in 5d orbitals of Eu^{2+} interacts strongly with the neighboring ions and the position of the 5d band also depends on the crystal field strength. Therefore the luminescence of Eu^{2+} can be adjusted with different local structure and crystal field. In this work, Eu^{2+} and Dy^{3+} codoped solid solution $\text{Ca}_x\text{Sr}_{2-x}\text{SiO}_4$ with different compositions was investigated in an attempt to explore its color-tuning capability.

Alkaline-earth silicates with better physical and chemical stability have been chosen as our host for Eu^{2+} and Dy^{3+} codoping. In this study, a series of $\text{Ca}_x\text{Sr}_{2-x}\text{SiO}_4$: Eu^{2+} , Dy^{3+} phosphors were synthesized in order to optimize the emission under a variety of Ca^{2+} and Sr^{2+} proportions. In addition, a detailed investigation of powder X-ray diffraction (XRD), photo-luminescence (PL) and thermoluminescence was carried out to address the relation between the structural and the luminescent properties.

2 Experimental

A series of $\text{Ca}_x\text{Sr}_{2-x}\text{SiO}_4$: Eu^{2+} , Dy^{3+} phosphors with different Ca^{2+} and Sr^{2+} proportions were synthesized by high-temperature solid-state reactions. CaCO_3 (A.R.), SrCO_3 (A.R.), SiO_2 (A.R.) and Eu_2O_3 (99.99%) and Dy_2O_3 (99.99%) were used as starting materials. Stoichiometric amounts of the raw materials have been mixed and thoroughly ground in an agate mortar, and then calcined at 1250 °C for 6 h in a reducing atmosphere (5% H_2 + 95% N_2) to obtain the powder samples.

To study the influence of $\text{Ca}^{2+}/\text{Sr}^{2+}$ ratio on $\text{Ca}_x\text{Sr}_{2-x}\text{SiO}_4$: Eu^{2+} , Dy^{3+} samples, Ca composition with $x = 0, 0.2, 0.4, 0.6, 0.8, 1.0, 1.2, 1.4, 1.6, 1.8, 2.0$ (molar ratio) respectively were prepared in the experiments. The crystal structures were analyzed by a MXP-AHF rotating anode X-ray diffractometer (Cu-K_α radiation). The XRD profiles were collected in the range of $10^\circ < 2\theta < 70^\circ$. Photoluminescence excitation (PLE) and emission (PL) spectra were characterized on a HITACHI 850 fluorescence spectrometer with a 150 W Xe lamp as an excitation source. Thermoluminescence was measured by heating the sample over a small metal plate and the emission intensity was monitored using a photomultiplier tube. Before starting the thermoluminescence measurement, few milligrams of sample was irradiated with 365 nm excitation.

3 Results and discussion

3.1 Phase and crystal structure analysis

Fig. 1 shows the XRD patterns of the $\text{Ca}_x\text{Sr}_{2-x}\text{SiO}_4$: 0.01 Eu^{2+} , 0.01 Dy^{3+} phosphors ($x = 0, 0.2, 0.4, 0.6, 0.8, 1.0, 1.2, 1.4, 1.6, 1.8$ and 2.0) produced by solid-state reaction synthesis at 1250 °C and the standard data of Sr_2SiO_4 (PDF-38271) and Ca_2SiO_4 (PDF-70388). It is obvious that changing the Ca/Sr ratio cannot get continuous solid-state solutions from Ca_2SiO_4 to Sr_2SiO_4 , while different phases with different crystal

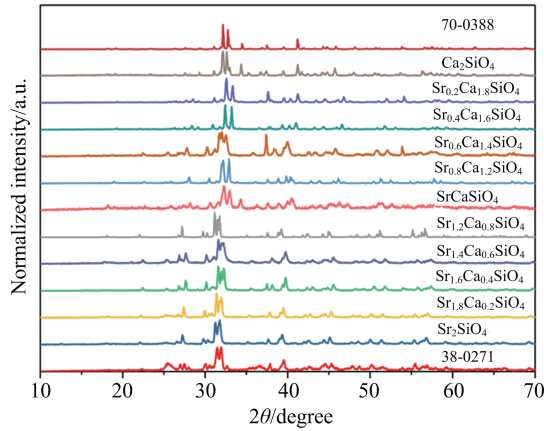


Fig.1 The XRD patterns of $\text{Ca}_x\text{Sr}_{2-x}\text{SiO}_4:0.01\text{Eu}^{2+}, 0.01\text{Dy}^{3+}$ samples and the standard data of Sr_2SiO_4 (PDF-38271) and Ca_2SiO_4 (PDF-70388)

reaction of raw materials is complete.

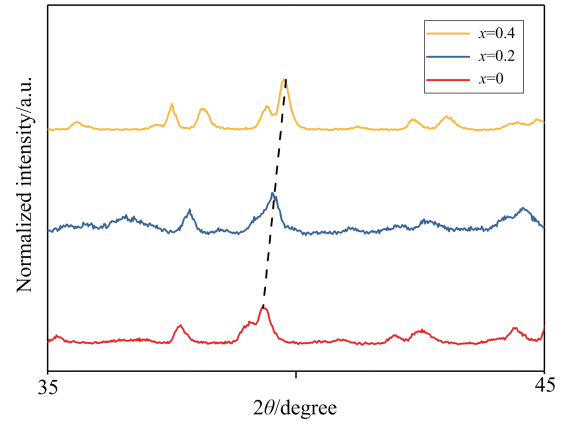


Fig.2 Magnified XRD patterns in the range of $0 \leq x \leq 0.4$ for $\text{Ca}_x\text{Sr}_{2-x}\text{SiO}_4:0.01\text{Eu}^{2+}, 0.01\text{Dy}^{3+}$ phosphors

structures formed. Orthorhombic α' - Sr_2SiO_4 and monoclinic β - Sr_2SiO_4 are two different crystallographic modifications of Sr_2SiO_4 . The β - and α' -forms of Sr_2SiO_4 have closely related crystal structures made of SiO_4 tetrahedra. The difference is just the small tilting in the SiO_4 tetrahedra (Td) which leads to the absence of a mirror plane that parallel to the (100) plane in the case of β - Sr_2SiO_4 ^[12,13]. In the lattice structure of α' - Sr_2SiO_4 and β - Sr_2SiO_4 , Sr^{2+} ions located at two different kinds of sites and their coordination numbers are 9 and 10 respectively^[14,15,16]. The introduction of Sr^{2+} ions increased the lattice parameters of the phosphors. As the concentration ratio of Ca^{2+} ions in the host was increased (x from $0 \rightarrow 0.4$), the main diffraction peaks were basically shifted to a larger angle, as demonstrated in Fig. 2, because the ionic radius of Ca^{2+} (0.10 nm) ions is smaller than Sr^{2+} (0.118 nm) ions. The level of Eu^{2+} doping has a strong influence on the phase formation of $\text{Sr}_2\text{SiO}_4:\text{Eu}^{2+}, \text{Dy}^{3+}$. If the Eu^{2+} concentration is small, $\text{Sr}_2\text{SiO}_4:\text{Eu}^{2+}, \text{Dy}^{3+}$ exists in the monoclinic β -phase. In our experiment, The crystal structures of $\text{Ca}_{2-x}\text{Sr}_x\text{SiO}_4:0.01\text{Eu}^{2+}, 0.01\text{Dy}^{3+}$ are divided into two groups, namely, β phase ($0 \leq x < 1$) and α' phase ($1 < x < 2$). Besides, no peaks of un-reacted SrCO_3 and SiO_2 are observed in XRD patterns, indicating that the

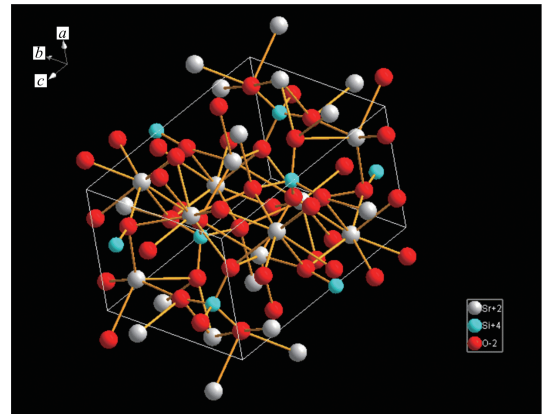


Fig.3 Schematic crystal structure diagrams of β - Sr_2SiO_4

Fig.4 presents the photoluminescence of the Sr-rich $\text{Ca}_x\text{Sr}_{2-x}\text{SiO}_4:0.01\text{Eu}^{2+}, 0.01\text{Dy}^{3+}$ phosphors with composition $x < 1$ under 365 nm excitation. As shown in the emission spectra, the intensity of the broadband $\text{Eu}^{2+} 5d \rightarrow 4f$ emission covering nearly whole visible wavelength range increased with Ca^{2+} concentration until $x = 0.4$. The shape of the Eu^{2+} emission band implies that there are different cation sites in the host for Eu^{2+} occupation. The extraordinary broadness of the Eu^{2+} emission band indicates a strong coupling between the host lattice and the Eu^{2+} ions, owing to the excited electrons in the outer 5d shell of the Eu^{2+} ions. The introduction of Ca in Sr-rich host causes the longer wavelength subband more prominent, thus leading to the observed red shift

of the peak position of the emission band. This result suggests that the Eu^{2+} sites with stronger crystal field strength increased with introduction of Ca in Sr-rich host.

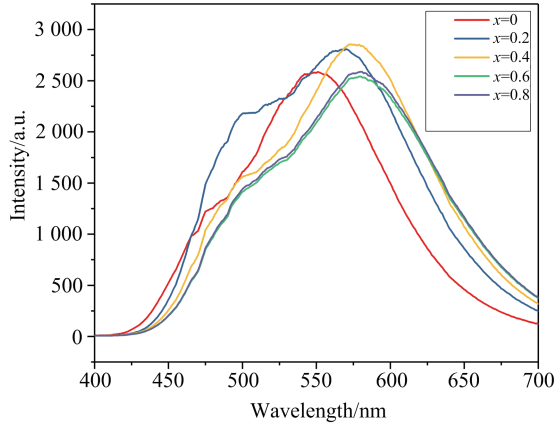


Fig.4 PL spectra of $\text{Ca}_x\text{Sr}_{2-x}\text{SiO}_4:0.01\text{Eu}^{2+}, 0.01\text{Dy}^{3+}$ ($x=0, 0.2, 0.4, 0.6$, and 0.8 , respectively) under 365 nm excitation

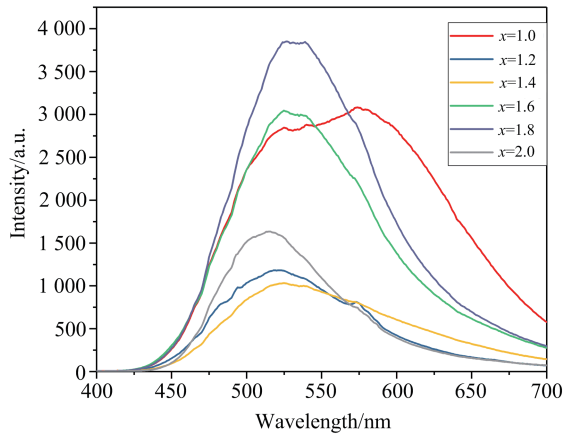


Fig.5 PL spectra of $\text{Ca}_x\text{Sr}_{2-x}\text{SiO}_4:0.01\text{Eu}^{2+}, 0.01\text{Dy}^{3+}$ ($x=1.0, 1.2, 1.4, 1.6, 1.8$ and 2.0 , respectively) under 365 nm excitation

Interestingly, the longer wavelength subband was gradually suppressed in the Ca-rich host $\text{Ca}_x\text{Sr}_{2-x}\text{SiO}_4:0.01\text{Eu}^{2+}, 0.01\text{Dy}^{3+}$ with $x > 1$, eventually leaving only the shorter wavelength green subband peaking around 520 nm, as shown in the PL spectra of Fig. 5. When carefully checking PL spectra in Fig. 5 for $x > 1$, it is found that the PL band at 520 nm keep unchanged with x increasing from 1 to 1.8. Only obvious blue shift is observed for $x = 2.0$, namely, the Ca_2SiO_4 :

$0.01\text{Eu}^{2+}, 0.01\text{Dy}^{3+}$ one. Because the radius of Eu^{2+} is very close to the radius of Sr^{2+} , when substituting Ca by Sr, it will cause the redistribution of Eu^{2+} in different sites.

The increasing difference of electro-negativity between the constituting cation and anion would lower the covalency, which enhances the interaction among outer-shell electrons [17]. When Sr^{2+} ions are substituted by Ca^{2+} ions in Sr_2SiO_4 , the barycenter of 5d energy levels of Eu^{2+} will be reduced because of the higher electro-negativity of Ca (1.00) than Sr (0.95), which leads to lower 5d level of Eu^{2+} and leads to a red-shift in the PL spectra [18]. The effective ionic radius in nine-fold coordination of Sr^{2+} (1.31 Å) is larger than Ca^{2+} (1.18 Å), resulting in the host lattice shrink [19]. The distance between the cation and the surrounding anion affects the crystal-field strength (Dq) significantly, i. e., Dq is proportion to R^{-5} [20]. The shorter Ca-O pairs bond-length than Sr-O pairs make Eu^{2+} ions experience stronger crystal-field in Ca-rich case, which contributes to lower-energy emission from $4f^65d^1$ energy level and a further red-shift as x increases.

In conclusion, a higher electro-negativity of Ca should reduce the difference of electro-negativity between Ca and O, and the covalency should increase, therefore the barycenter of 5d levels (not $4f^65d^1$ energy levels) reduces. The substitution of Sr by Ca will lead to the increase of crystal field splitting of 5d levels. These two reasons lead to the red shift of PL band, which can be used to explain the result for $x < 1$. Therefore, an irregular overall red-shift of the emission peak could be discerned with the increase of the Ca portion in the composition.

Fig.6 shows the excitation spectra (monitored at 502 nm) (a) and the emission spectra (excited at 365 nm) (b) of $\text{Ca}_x\text{Sr}_{2-x}\text{SiO}_4:0.01\text{Eu}^{2+}, 0.01\text{Dy}^{3+}$ ($x = 0.6$), respectively. The excitation spectra exhibited a broad band between 220 and 400 nm. This broad band has two center peaks. The

position of the two peaks situated at approximately 275nm and 325nm, respectively. From these results, it implied an efficient energy transfer from

the host to Eu^{2+} . The efficient energy transfer makes it difficult to observe the emission from Dy^{3+} .

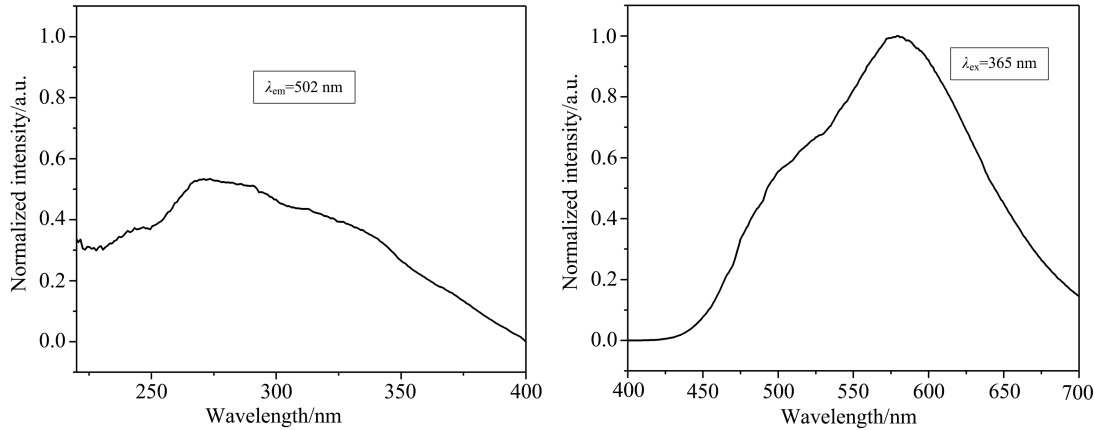


Fig.6 PLE(monitored 502 nm emission) and PL (excited at 365 nm) spectra of $\text{Ca}_x\text{Sr}_{2-x}\text{SiO}_4:\text{Eu}^{2+}, \text{Dy}^{3+}$ ($x=0.6$)

In pure $\text{Sr}_2\text{SiO}_4:\text{Eu}^{2+}$, good persistent luminescence from Eu^{2+} can be procured by codoping Dy^{3+} , which is responsible for sufficient trap supply which is necessary for the long afterglow performance. However, the duration and the intensity of the persistent luminescence were rapidly degraded with substitution of Sr by Ca in the host, as revealed by the long afterglow measurements shown in Fig. 7. The shape of the long afterglow curves for these three samples $\text{Ca}_x\text{Sr}_{2-x}\text{SiO}_4:0.01\text{Eu}^{2+}, 0.01\text{Dy}^{3+}$ ($x=0, 0.4, 0.8$) is dissimilar, which suggests different depth of electron traps in these three phosphors. This tells us the fact that the crystallographic of the three phosphors are a little bit different. It consists with our previous argument. The different intensities of the afterglow intensity imply different density or trapping efficiency for the traps. However, the detailed persistent luminescence mechanism is not known. Very likely Dy^{3+} ions are involved in electron trapping, and for this reason the persistent emission is stronger when Dy^{3+} is added. Dy^{3+} ions can replace the Sr^{2+} ions, which may promote the formation of defects such as oxygen vacancies which could act as electron traps [21]. The persistent luminescence totally disappeared in the Ca-rich samples when $x>1.0$. This phenomenon is

noteworthy in that for most of alkaline earth long afterglow phosphors with similar host structure, the Sr-based host will yield better persistent luminescence performance than that of Ca-based host. To further illustrate this condition, we measured the thermoluminescence curves of $\text{Ca}_x\text{Sr}_{2-x}\text{SiO}_4:0.01\text{Eu}^{2+}, 0.01\text{Dy}^{3+}$ (Fig 8.)

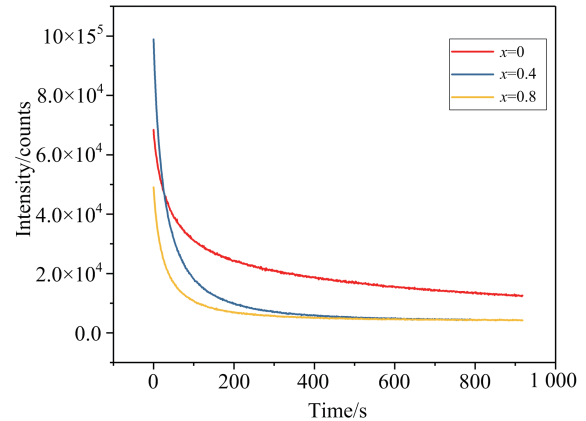


Fig.7 The long afterglow curves of $\text{Ca}_x\text{Sr}_{2-x}\text{SiO}_4:0.01\text{Eu}^{2+}, 0.01\text{Dy}^{3+}$ ($x=0, 0.4, 0.8$)

From Fig.8, it can be found that the depth of the trap levels changed remarkably with the increased concentration of Ca^{2+} . In Sr-rich samples with $x<1.0$, there existed only one thermoluminescence peak located between 50 °C and 200 °C, though the precise peak position is

varied for different samples. But in Ca-rich samples with $x > 1.0$, another peak emerged at above 350°C. Meanwhile, the non-monotonous peak shifting in the thermoluminescence curves is in accord with the PL. It can be inferred from the Fig. 8 that in Sr-rich samples with $x < 1.0$, the electrons will be captured mainly by the shallow trap, which are favorable for the persistent luminescence at room temperature, while in Ca-rich samples with $x > 1.0$, the electrons could be channeled to the much deeper trap levels, which are detrimental for the persistent luminescence. It can explain why the persistent luminescence property became worse when we increased the concentration of Ca^{2+} in the host. The thermoluminescence of $\text{Sr}_2\text{SiO}_4:\text{Eu}^{2+}, \text{Dy}^{3+}$ was in the appropriate temperature range of 70-150 °C, accounting for its good persistent luminescence property.

The Commission International de l'Eclairage France(CIE) x-y color coordinates diagram of the $\text{Ca}_x\text{Sr}_{2-x}\text{SiO}_4:0.01\text{Eu}^{2+}, 0.01\text{Dy}^{3+}$ phosphors are

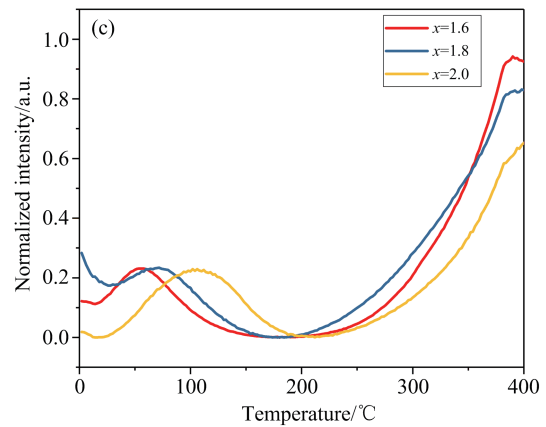
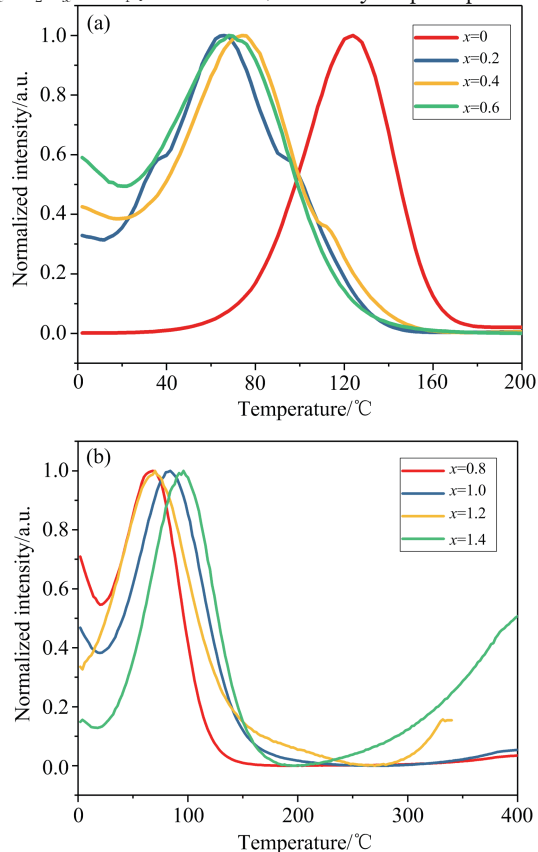


Fig.8 The thermoluminescence curves of $\text{Ca}_x\text{Sr}_{2-x}\text{SiO}_4:0.01\text{Eu}^{2+}, 0.01\text{Dy}^{3+}$

shown in Fig.9. From Fig.9, it is observed that the color coordinates of present phosphors fall within the yellow-greenish light region. By changing the concentration ratio of Ca^{2+} and Sr^{2+} ions of these phosphors, we can get different light which we need.

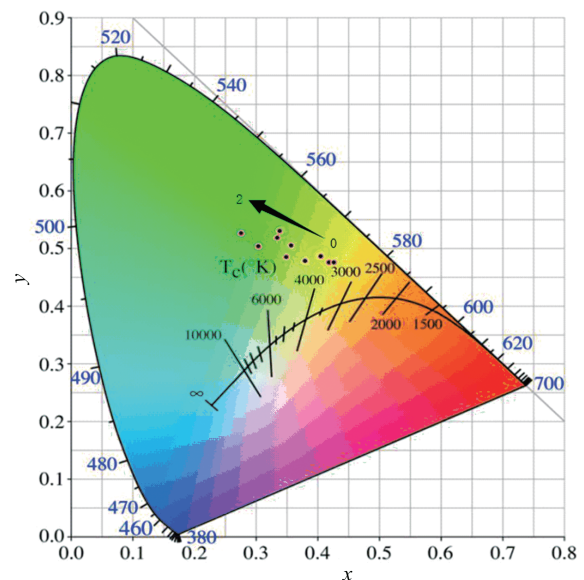


Fig.9 CIE chromaticity diagram for samples $\text{Ca}_x\text{Sr}_{2-x}\text{SiO}_4:0.01\text{Eu}^{2+}, 0.01\text{Dy}^{3+}$ ($x=0, 0.2, 0.4, 0.6, 0.8, 1.0, 1.2, 1.4, 1.6, 1.8, 2.0$ respectively) excited at 365 nm

4 Conclusions

A series of $\text{Eu}^{2+}, \text{Dy}^{3+}$ co-doped $\text{Ca}_x\text{Sr}_{2-x}\text{SiO}_4$ phosphors have been successfully synthesized by the solid-state reaction method and their structural

and luminescence properties were investigated. The structure of the synthesized phosphors are crystallized in monoclinic. From the photoluminescence spectra, we can get that this phosphor is efficiently excited by light which wavelength ranges from 250 to 400 nm. This kind of phosphor can emit intensely yellow-green light with a broad band which peaks at around 550

nm. We also observed the unusual spectroscopic properties that the spectral shape and the peak shift were non-linearly dependent on the composition in solid-solution silicates $\text{Ca}_x\text{Sr}_{2-x}\text{SiO}_4:0.01\text{Eu}^{2+}, 0.01\text{Dy}^{3+}$. The phenomena can be further exploited in the development of new color-tunable luminescent materials.

参 考 文 献

- [1] X. Huang, S. Han, W. Huang, X. Liu, *Chem. Soc. Rev.* **42** (2013) 173.
- [2] X. Liu, R. Deng, Y. Zhang, Y. Wang, H. Chang, L. Huang, X. Liu, *Chem. Soc. Rev.* **44** (2015) 1479.
- [3] F. Wang, X. Liu, *Chem. Soc. Rev.* **38** (2009) 976.
- [4] F. Auzel, *Chem. Rev.* **104** (2004) 139.
- [5] P. Haritha, I. R. Martín, C. S. Dwaraka Viswanath, N. Vijaya, K. Venkata Krishnaiah, C. K. Jayasankar, D. Haranath, V. Lavin, V. Venkatramu, *Opt. Mat.* **70** (2017) 16.
- [6] R. Rajeswari, C. K. Jayasankar, D. Ramachari, S. Surendra Babu, *Ceram. Int.* **39** (2013) 7523.
- [7] Y. Shimizu, K. Sakano, Y. Noguchi, T. Moriguchi, Light Emitting Device Having a Nitride Compound Semiconductor and a Phosphor Containing a Garnet Fluorescent Material, U. S. Patent 59998925, 1999.
- [8] Y. Hu, W. Zhuang, H. Ye, D. Wang, S. Zhang, X. Huang, *J. Alloy. Compd.* **390** (2005) 226.
- [9] X. He, M. Guan, N. Lian, J. Sun, T. Shang, *J. Alloy. Compd.* **492** (2010) 452.
- [10] H. Y. Jiao, Y. H. Wang, *Appl. Phys. B* **98** (2010) 423.
- [11] G. Blasse, B. C. Grabmaier, *Luminescent Materials*, Springer, Berlin, 1994.
- [12] J. H. Lee and Y. J. Kim, *J. Ceram. Proc. Res.*, **10** (2009) 81.
- [13] X. Sun, J. Zhang, X. Zhang, Y. Luo, and X. Wang, *J. Rare Earths*, **26** (2008) 421.
- [14] N. Lakshminarasimhan, U. V. Varadaraju, *J. Electrochem. Soc.*, **152** (2005) H152.
- [15] M. Catti, G. Gazzoni, G. Ivaldi, *Acta Cryst.*, **C39** (1983) 29.
- [16] B. G. Hyde, J. R. Sellar, L. Stenberg, *Acta Cryst.*, **423** (1986) B42.
- [17] C. B. Cheng, L. T. Fang, Z. D. Zhang, Y. H. Xiao, S. J. Lei, *J. Phys. Chem. C* **115** (2011) 1708.
- [18] H. S. Jang, H. Y. Won, S. Vaidyanathan, D. H. Kim, D. Y. Jeon, *J. Electrochem. Soc.* **156** (2011) 138.
- [19] R. D. Shannon, *Acta Crystallogr. Sect. A* **32** (1976) 751.
- [20] T. Kanou, *Handbook of Phosphors*, Ohm Press, Tokyo 1987.
- [21] D. Dutczak, A. Milbrat, A. Katelnikovas, A. Meijerink, C. Ronda, T. Jüstel, *Journal of Luminescence*, **132** (2012) 2398.